CHEMISTRY
A EUROPEAN JOURNAL

DOI: 10.1002/chem.200600651

Hydrogen-Bonded Oligo(*p*-phenylenevinylene) Functionalized with Perylene Bisimide: Self-Assembly and Energy Transfer

Jian Zhang,[a] Freek J. M. Hoeben,[b] Maarten J. Pouderoijen,[b] Albertus P. H. J. Schenning,*[b] E. W. Meijer,*[b] Frans C. De Schryver,[a] and Steven De Feyter*[a]

Abstract: We describe the synthesis, supramolecular ordering on surfaces and in solution, and photophysical characterization of **OPV4UT-PERY**, an oligo(*p*-phenylenevinylene) (OPV) with a covalently attached perylene bisimide moiety. In chloroform, the molecule forms dimers through quadruple hydrogen bonding of the ureido-*s*-triazine array. This is supported by scanning tunneling microscopy (STM) studies, which reveal dimer formation at the liquid (1,2,4-trichlorobenzene)/solid (graphite) interface. Moreover, contrast reversal in bias-dependent STM imaging provides information on the ordering and different electronic properties of the oligo(*p*-phenylenevinylene) and perylene bisimide moieties. In dodecane, the molecule self-assembles into H-type aggregates that are still soluble as a result of the hydrophobic shell formed by the dodecyloxy wedges. The donor–acceptor molecule is characterized by efficient energy transfer from the photoexcited OPV to the perylene bisimide. Mixed assemblies with analogous OPVs lacking the perylene bisimide unit have been prepared in dodecane solution and energy transfer to the incorporated perylene bisimides has been studied by fluorescence spectroscopy.

Keywords: energy transfer · oligo(*p*-phenylenevinylene) · perylene bisimides · scanning tunneling microscopy · self-assembly · supramolecular chemistry

Introduction

Supramolecular control over dye arrangement is important for improving the performance of existing optoelectronic devices and for creating new dye-based materials with tunable optical and electronic properties.[1,2] Consequently, considerable effort is being focused on the structural modification of organic dyes in order to program their self-organization. These studies have generated a wealth of knowledge resulting in the design of a variety of materials with intriguing properties.[2] Hydrogen bonds are ideal noncovalent interactions to construct supramolecular architectures since they are highly selective and directional, not only in solution but also on surfaces.[3,4,5] Synthetic hydrogen-bonded donor–acceptor dyads have been successfully used to unravel biological light-harvesting phenomena.[6] Such assemblies are not only important for addressing fundamental questions in chemical biology, but are also of great interest in the design of devices in which electron and energy transfer play an important role. However, apart from the well-documented examples of supramolecular donor–acceptor dyads, the next level of hierarchy, extended multicomponent assemblies in solution, has been less investigated.[1] On surfaces, only a few reports deal with high-spatial resolution studies on the ordering and electronic properties of supramolecular donor–acceptor dyads or triads.[7,8]

Perylene bisimides and oligo(*p*-phenylenevinylene)s (OPVs) are attractive compounds for the construction of supramolecular architectures with photophysical functionali-

[a] Dr. J. Zhang, Prof. F. C. De Schryver, Dr. S. De Feyter
Division of Molecular and Nano Materials
Laboratory of Photochemistry and Spectroscopy
Katholieke Universiteit Leuven,
Celestijnenlaan 200 F, 3001 Leuven (Belgium)
Fax: (+32) 16-327-990
E-mail: Steven.DeFeyter@chem.kuleuven.be

[b] Dr. F. J. M. Hoeben, M. J. Pouderoijen, Dr. A. P. H. J. Schenning, Prof. Dr. E. W. Meijer
Laboratory of Macromolecular and Organic Chemistry
Eindhoven University of Technology
P.O. Box 513, 5600 MB Eindhoven (The Netherlands)
Fax: (+31) 40-245-1036
E-mail: a.p.h.j.schenning@tue.nl
e.w.meijer@tue.nl

Supporting information for this article is available on the WWW under http://www.chemeurj.org/ or from the author.

ty.[9] Perylene bisimides have been extensively studied, for example, as liquid crystals,[10] in (supramolecular) donor–acceptor systems,[11] as foldamers,[12] or as components in solar cells.[13] Only recently, their two-dimensional self-organization on surfaces was addressed.[8c,14,15] Combining our earlier work on hydrogen-bonded OPVs[15,16] with our studies on OPV–perylene bisimide donor–acceptor systems,[8a,b,17] we now report on the direct functionalization of an OPV derivative with perylene bisimide (**OPV4UT-PERY**) (Scheme 1). In this way, a unique building block is obtained, composed of an OPV unit covalently linked to perylene bisimide through a flexible linker. The system is capable of a hierarchical assembly by hydrogen bonding and π–π interactions. These assemblies have been characterized by photophysical methods in solution and "electronically" (at the liquid/solid interface) by scanning tunneling microscopy (STM). In addition to the pure system, mixtures with **OPV*n*UT** derivatives (Scheme 1) have been studied.

Results and Discussion

Synthesis and characterization: Scheme 1 shows the synthesis of **OPV4UT-PERY** comprising covalently linked OPV and perylene bisimide. By using this approach, OPV in principle can be easily functionalized with any desired chromophore. 1,7-Bis(3,5-di-*tert*-butylphenoxy)perylene-3,4:9,10-tetracarboxylic dianhydride was treated with 1-ethylpropylamine in refluxing dry *N*,*N*-dimethylacetamide (DMA) to yield a mixture of **1** and its disubstituted analogue **1b** (used as a reference compound). After separating these two compounds, **1** was rigorously purified by column chromatography to ensure that only the 1,7-isomer remained.[18] Subsequent coupling of **1** with excess 1,5-pentanediamine in dry DMA yielded asymmetric perylene bisimide **2**. This amine was further converted to the corresponding isocyanate **3** by reaction with di-*tert*-butyl tricarbonate in dichloromethane.[19] Finally, coupling of **OPV4T** with **3** in refluxing pyridine furnished **OPV4UT-PERY**, which was rigorously purified by column chromatography and preparative size-exclusion chromatography and was fully characterized.

^{1}H NMR experiments in $CDCl_3$ clearly indicated the dimerization of **OPV4UT-PERY** through intermolecular hydrogen bonding. The hydrogen-bonding pattern appeared to be slightly shifted with respect to the previously reported dimer of **OPV4UT** which has a dimerization constant of $K_{dim} = 2.1 \times 10^{-4}\,M^{-1}$ in chloroform.[16] The resonances of the hydrogen-bonded protons of the ureido-*s*-triazine array, which appear at $\delta = 9.3$, 9.9, and 10.2 ppm for **OPV4UT**, were found at $\delta = 9.2$, 9.6, and 9.8 ppm for **OPV4UT-PERY** at similar concentrations in CD_3Cl (Figure 1) indicating that its dimerization constant is lower than that of **OPV4UT**.

Self-assembly at the liquid/solid interface: **OPV4UT-PERY** was dissolved in 1,2,4-trichlorobenzene and a drop of the solution (0.5 mg mL^{-1}) was placed on the surface of freshly

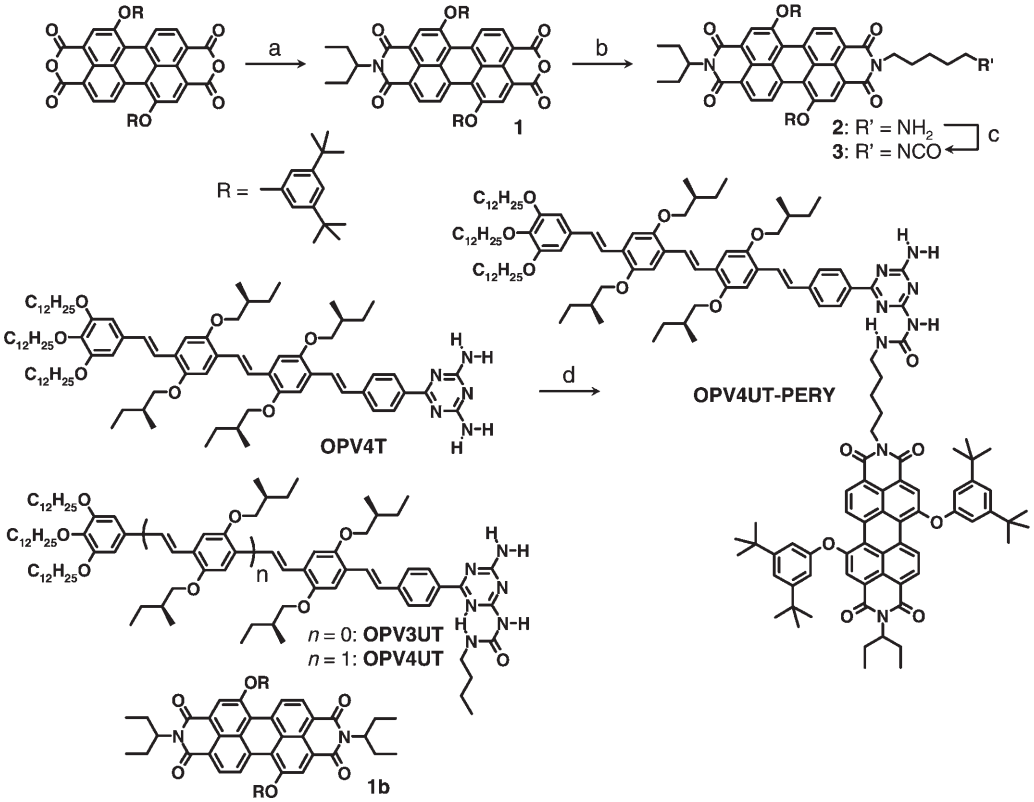

Scheme 1. Synthesis of **OPV4UT-PERY**. Reagents and conditions: a) 1-ethylpropylamine, $Zn(OAc)_2$, DMA, reflux, 3 h, 28%; b) 1,5-pentanediamine, $Zn(OAc)_2$, DMA, 50 °C, 2 h, 65%; c) di-*tert*-butyl tricarbonate, dichloromethane, 20 °C, 10 min, 100%; d) **3**, pyridine, reflux, 16 h, 15%. Compounds **OPV3UT**, **OPV4UT**, and perylene bisimide **1b** were used in optical reference studies.

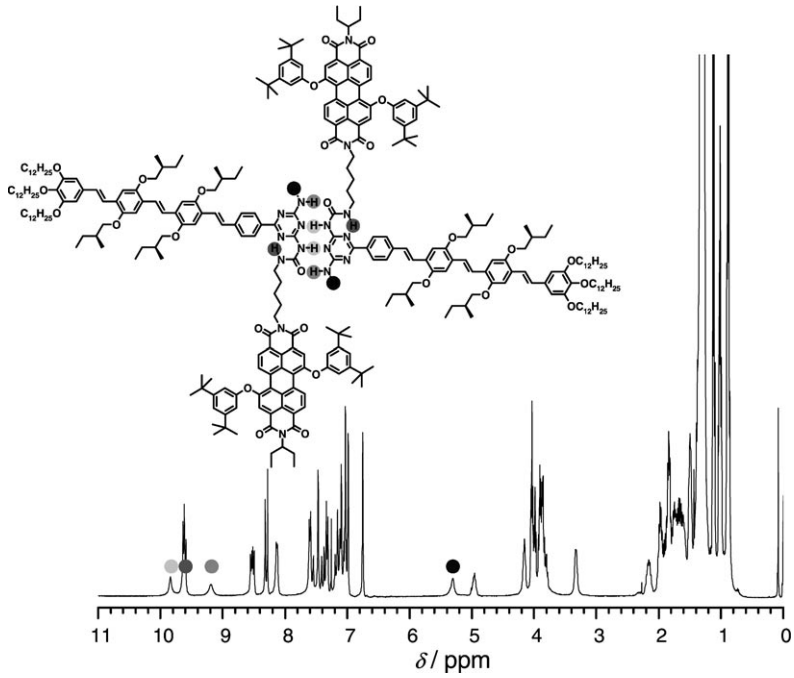

Figure 1. ^{1}H NMR spectrum of **OPV4UT-PERY** in $CDCl_3$ at room temperature. Relevant protons of the ureido-*s*-triazine units in the dimer are highlighted.

though individual alkyl chains are not visible, modeling shows that they are located in the dark, broad "gaps", and are interdigitated.

Interestingly, the side-to-side distance between adjacent bright rods is much larger than observed for **OPV4UT** (2.7 nm versus 2.0 nm).[22] Another difference is the orientation of the long axis of the bright rods with respect to the row axis, which is nearly perpendicular for **OPV4UT-PERY** but rotated by almost 45° for **OPV4UT**. Finally, in the case of **OPV4UT-PERY**, the width of the bright rods often exceeds the expected OPV width. These elements strongly indicate that the PERY units are adsorbed between the dimers rather than on top of the OPV units.

cleaved highly oriented pyrolytic graphite. 1,2,4-Trichlorobenzene and not chloroform was selected because of its low vapor pressure which facilitates the experiments at the liquid/solid interface as no closed cell is used.[20] In addition, under similar conditions, successful self-assembly and STM imaging of **OPV4UT** have previously been achieved.[15d] Under these conditions, a substantial fraction of the molecules appear as hydrogen-bonded dimers in solution (vide supra). The STM tip was then immersed in the solution and the surface scanned. After a while, the images revealed a particular contrast which indicates the presence of immobilized molecules. Figure 2 shows such a large-scale STM image. The image shows relatively ordered domains with parallel bright rods that are unequally spaced. They appear to have dimerized as the end-to-end distance between the rods changes in an alternating fashion, leading to small and large "gaps". The bright rods of the dimers are often but not always in line (depending on the rod's long axis) (see also Figure 3). The point defects (missing rods) indicate that a rod corresponds to one molecule. However, a rod does not represent the complete molecule, only the OPV part. This is supported by the fact that 1) the length of a bright rod agrees well with the expected length of the OPV unit (2.56 ± 0.03 nm), 2) dimerization of the rods is also observed for **OPV4UT**, the model compound previously investigated,[15d] and 3) a substantial fraction of molecules already exist as dimers in solution.[21] Therefore, it is safe to conclude that the OPV units of the physisorbed molecules are linked to each other by hydrogen bonding through the self-complementary ureido-*s*-triazine arrays. Differences in the off-set between the OPV units of the hydrogen-bonded dimers can be attributed to conformational aspects.[15d] Although individual alkyl chains are not visible, modeling shows that they are located in the dark, broad "gaps", and are interdigitated.

It proved extremely difficult to image the perylene bisimide unit, probably because it is not adsorbed as strongly on the graphite surface, hence it has a high mobility. We tentatively assigned the low-contrast features between adjacent OPV dimers, as observed in Figure 3, to the perylene bisimide units. Our previous studies involving bias-dependent imaging and scanning tunneling spsctroscopy (STS) measurements of covalently linked OPV–perylene bisimide–OPV systems showed that the perylene bisimide and OPV moiet-

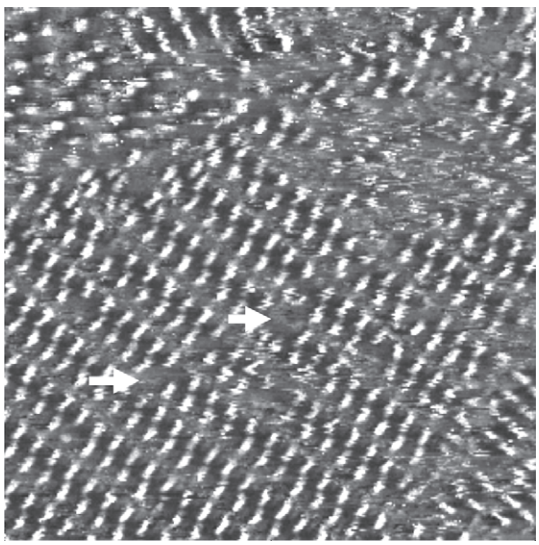

Figure 2. STM image showing an **OPV4UT-PERY** monolayer on graphite, physisorbed from a concentrated 1,2,4-trichlorobenzene solution (0.5 mg mL^{-1}). The arrows indicate vacancies in the 2D lattice. The image size is 58×58 nm^2. $I_{set} = 0.25$ nA, $V_{bias} = -1.16$ V.

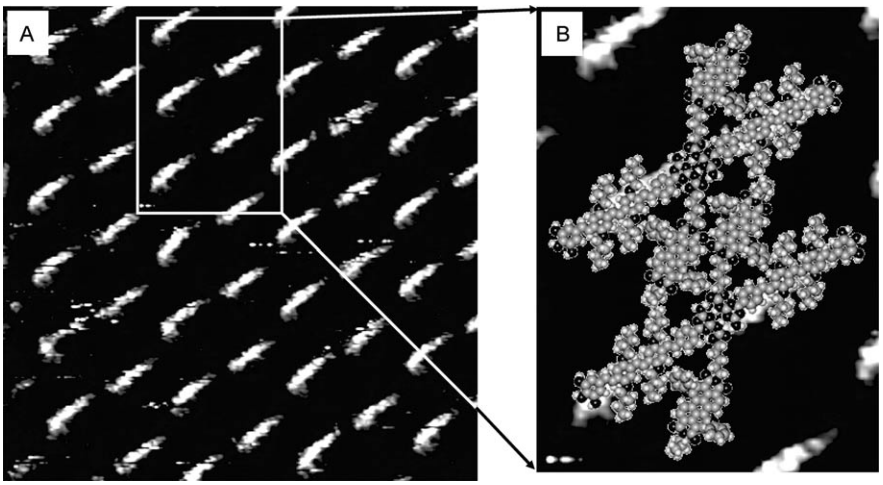

Figure 3. a) STM image showing an **OPV4UT-PERY** monolayer on graphite, physisorbed from a 1,2,4-trichlorobenzene solution. Image size is 25 nm × 25 nm^2. I_{set} = 0.12 nA, V_{bias} = −1.48 V. b) Enlarged image of the indicated area in (a) with molecular model.

ies exhibit opposite rectifying behavior.[8a,b] At a high negative sample bias (electrons tunneling from the substrate to the tip) the OPV units appeared brighter than the perylene bisimide moieties: the tunneling process is more efficient through the OPV part than through the perylene bisimide core. At a high positive bias voltage (electrons tunneling from the tip to the substrate), the opposite situation was observed: the perylene bisimide units appeared brighter (a higher tunneling efficiency) than the OPV units. This was explained by the different degree of involvement of the molecular frontier orbitals in the tunneling process. At highly negative bias voltages, the highest occupied molecular orbital (HOMO) of the OPV unit is considered to support tunneling while at high positive bias voltages, the lowest unoccupied molecular orbital (LUMO) of the perylene bisimide unit is the key orbital.[8a,b] So eventually, by using bias-dependent STM measurements and STS of monolayers of **OPV4UT-PERY**, we anticipated that it should be possible to locate the perylene bisimide units and to distinguish them from the OPV rods.

Figure 4a and 4b are STM images obtained sequentially at the exact same location, but at negative and positive sample biases, respectively. There is a clear bias-dependent reversal of the image contrast. In analogy with the compounds previously studied, we assign the bright areas in Figure 4a to the OPV rods while the more square-like bright spots in Figure 4b indicate the location of the PERY units.[23] The images suggest that the perylene bisimide moieties of adjacent hydrogen-bonded dimers are in close proximity, since on average a single bright spot is observed for every hydrogen-bonded **OPV4UT-PERY** dimer. Attempts to record reproducible STS curves on top of these molecules failed, since the monolayers are relatively unstable and especially as the PERY units are not strongly adsorbed. Therefore, we tried to form mixed monolayers of **OPV4UT-PERY** and **OPV4UT** in order to increase monolayer stability, however, mixed monolayers were not formed. Only **OPV4UT** monolayers were observed regardless of the excess of **OPV4UT-PERY** in the liquid phase, which stresses their different adsorption affinities: the bulky nature of the PERY groups has a negative impact on monolayer stability.

Optical properties and self-assembly in solution: Knowing the molecular structure of the dimer at a surface we studied the self-assembly properties of **OPV4UT-PERY** in various solvents using UV/Vis, CD, and fluorescence spectroscopy. In chloroform (10^{-6} M, Figure 5a) the molecule displays the characteristic π–π* transition of the OPV moiety at λ_{max} = 443 nm, corresponding to previous observations with **OPV4UT**.[16] The perylene bisimide $S_1 \leftarrow S_0$ transition is de-

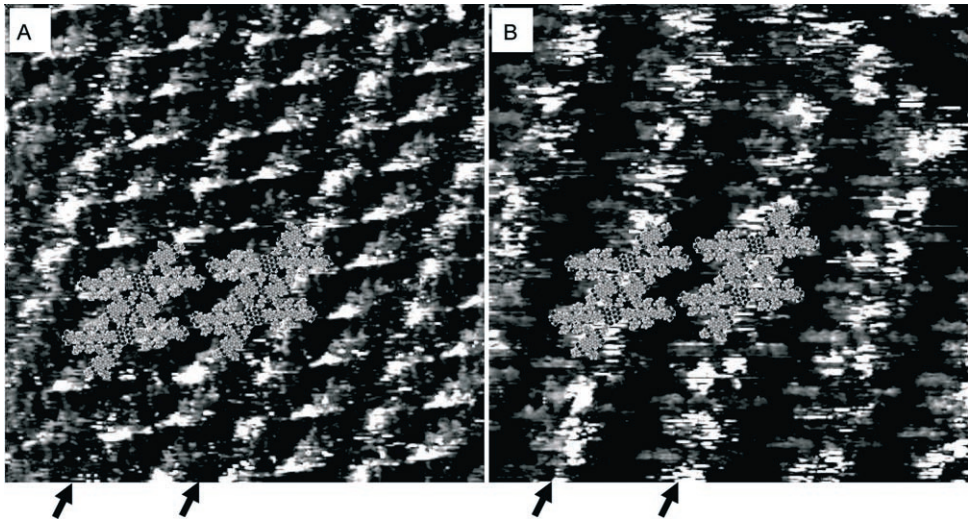

Figure 4. Bias-dependent imaging of the same area (except for a small drift) of an **OPV4UT-PERY** monolayer at the 1,2,4-trichlorobenzene/graphite interface. a) I_{set} = 115 pA, V_{bias} = −1.37 V, showing the OPV units as brighter areas, and b) I_{set} = 115 pA, V_{bias} = +1.22 V, showing the perylene bisimide units as brighter areas. Image sizes are 25 nm × 25 nm. The models illustrate molecular packing and dimer formation. The arrows indicate corresponding sites.

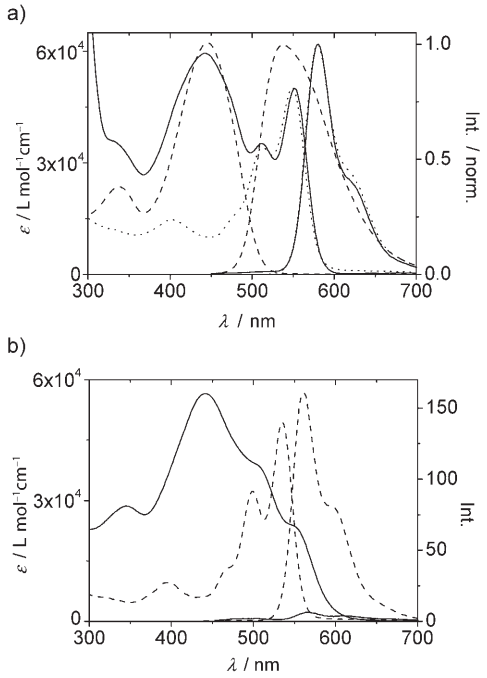

Figure 5. UV/Vis and emission spectra of a) **OPV4UT** (dashed lines), **1b** (dotted lines), and **OPV4UT-PERY** (solid lines) in chloroform and b) **1b** (dashed lines) and **OPV4UT-PERY** (solid lines) in dodecane. For all compounds, concentration $=10^{-6}$ M and $\lambda_{exc}=440$ nm.

tected at $\lambda_{max}=552$ nm, accompanied by a lower intensity vibrational band at $\lambda=512$ nm. As expected, fluorescence spectroscopy reveals complete quenching of OPV fluorescence, which is normally centered at around $\lambda_{em}=536$ nm. Strong perylene bisimide luminescence at $\lambda_{em}=580$ nm is indicative of efficient energy transfer from the OPV moiety to perylene bisimide, since at this excitation wavelength ($\lambda_{exc}=$ 440 nm) the OPVs are predominantly excited. At 10^{-6} M, **OPV4UT-PERY** is predominantly present in its monomeric form and consequently intramolecular energy transfer will dominate (intermolecular energy transfer can also occur when **OPV4UT-PERY** is present in its hydrogen-bonded dimer form). OPV fluorescence quenching (quenching factor, $Q_{OPV}\approx 70$ at $\lambda_{em}=536$ nm in comparison with **OPV4UT**, determined in a reference experiment), together with an **OPV4UT** fluorescence lifetime of $\tau=1.9$ ns,[24] yields a lower limit for the energy transfer rate of $k_{ENT}=3.6\times10^{10}$ s^{-1}.[25] The strong perylene bisimide luminescence moreover suggests that the relatively large distance between the two chromophores precludes electron transfer from donor to acceptor (vide infra). Addition of the UV/Vis spectra of reference compounds **OPV4UT** and **1b** in chloroform (10^{-6} M) reproduces the **OPV4UT-PERY** absorption spectrum, although the OPV π–π* transition seems to have lost some oscillator strength. This implies the absence of electronic communication between the donor and acceptor moieties in the ground state, which is expected because of the isolating pentamethylene linker. The fluorescence spectra of the reference compounds confirm the total loss of OPV fluorescence for **OPV4UT-PERY**.

In an apolar environment like dodecane (10^{-6} M, Figure 5b) the optical spectra are drastically different. The perylene bisimide absorptions decrease in favor of a new absorption band at around $\lambda_{max}=508$ nm, which becomes its most dominant transition, and at $\lambda=550$ nm with a weak absorption shoulder emerging at around $\lambda=600$ nm. This hypsochromic shift has been reported in the literature and has been attributed to intermolecular perylene bisimide aggregation into H-type aggregates.[26] While the dominant transition to the highest excitonic band (carrying the highest oscillator strength) is observed at $\lambda_{max}=508$ nm, vibronic coupling allows a symmetry-forbidden transition to the lowest excitonic state at $\lambda=550$ nm and further into the red region of the spectrum. Face-to-face packing of the optical transition dipoles should cause perylene bisimide fluorescence to decrease, in line with exciton theory. Indeed, while OPV luminescence is still almost indiscernible, perylene bisimide fluorescence has shifted to $\lambda_{em}=566$ nm and is almost completely quenched.[27] Surprisingly, in CD spectroscopy, no Cotton effect could be observed for either OPV or perylene bisimide at any concentration, indicating that self-assembly occurs in a fashion lacking the preferred handedness of a supramolecular structure. This raises serious questions about the internal structure of the assemblies that are formed. Compared with the butyl chains in **OPV4UT**, the perylene bisimide moiety is rather bulky and in order for **OPV4UT-PERY** to pack in a similar fashion to **OPV4UT**, the perylene bisimides should reside in the interior of a helical **OPV4UT** assembly.[28] Apparently, such a double-cable type of packing is sterically too demanding for the system.[29] On the other hand, the flexibility incorporated into the molecule through the pentyl spacer may simply leave the system with a severe lack of preorganization necessary for the formation of highly organized assemblies.

The stability of the supramolecular architectures formed by **OPV4UT-PERY** was investigated by using temperature-dependent UV/Vis and fluorescence measurements in dodecane (10^{-6} M, $\lambda_{exc}=440$ nm, Figure 6). Upon increasing the temperature, the shape of the perylene bisimide absorption changes to the shape of the absorption in chloroform, accompanied by the disappearance of the red-shifted shoulder at around $\lambda=600$ nm. The position of the OPV $S_2\leftarrow S_0$ absorption maximum, which is a sensitive probe for intermolecular aggregation,[16] shifts from 344 to 333 nm. Perylene bisimide fluorescence is restored at high temperatures and exhibits a hypsochromic shift to $\lambda_{em}=560$ nm, while its red-shifted shoulder diminishes (Figure 6b, inset). From these changes it is apparent that the assemblies dissociate into molecularly dissolved monomers and hydrogen-bonded dimers at elevated temperatures. This transition from aggregates to molecularly dissolved species occurs at around 45 °C according to both experimental techniques. Moreover, the concurrently observed spectral changes stemming either from the OPV or the perylene bisimide chromophore indicate the simultaneous disassembly of both moieties.

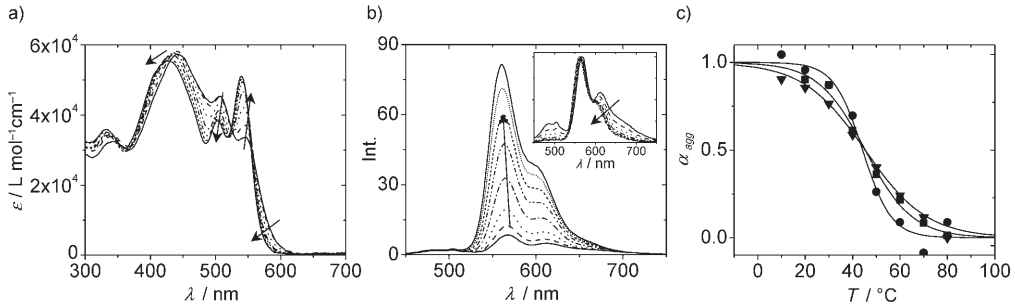

Figure 6. Temperature-dependent a) UV/Vis and b) fluorescence measurements on **OPV4UT-PERY** in dodecane (10^{-6} M, $\lambda_{exc}=440$ nm, normalized in the inset). The arrows indicate a temperature increase from 10 to 80 °C. c) The fraction of aggregated species as a function of temperature based on UV/Vis [perylene bisimide absorption at $\lambda=503$ nm (■) and the position of the OPV $S_2\leftarrow S_0$ maximum (●)] and perylene bisimide photoluminescence [$\lambda_{em}=560$ nm (▼)]. Lines to guide the eye.

Since the quantum yield of perylene bisimide luminescence decreases drastically in dodecane, the possibility of an additional electron-transfer process in the co-assembled state was assessed using femtosecond photoinduced absorption (PIA) measurements (5×10^{-5} M, see the Supporting Information). When the sample was excited at $\lambda_{exc}=455$ nm, however, the differential transmission signal probed at $\lambda=1450$ nm showed no appreciable amount of OPV radical-cation formation.[17a] From this it is safe to conclude that the photoluminescence quenching observed in dodecane is merely a consequence of perylene bisimide aggregation. The absence of electron transfer, moreover, suggests a substantial distance between the OPV and perylene bisimide units in the co-assembled state and excludes an alternating donor–acceptor stacking geometry.[30]

Mixed assemblies: Optical changes upon heterodimer formation of **OPV4UT-PERY** with **OPV3UT** and **OPV4UT** were investigated in chloroform (Figure 7, **OPV*n*UT** concentration fixed at 1.9×10^{-5} M). From the observed quenching behavior of both systems, it is clear that heterodimer formation leads to strong quenching of **OPV*n*UT** fluorescence (at $\lambda_{em}=515$ nm for **OPV3UT** and $\lambda_{em}=535$ nm for **OPV4UT**). Concomitantly, perylene bisimide luminescence arises at $\lambda_{em}=580$ nm due to energy transfer in the hydrogen-bonded complexes and direct excitation at increased acceptor incorporation.[31] Fluorescence quenching (Figure 7c) is similar for both systems, probably as a result of the relatively small difference in emission wavelength of **OPV3UT** and **OPV4UT** and the excellent Förster overlap between the luminescence of the two donors and perylene bisimide absorption. When comparing the quenching efficiency with that for the **OPV3UT/OPV4UT** system in chloroform, the relatively poor Förster overlap between **OPV3UT** luminescence and **OPV4UT** absorption is expressed in a less efficient quenching.

Similar titration experiments were performed in dodecane (Figure 8, **OPV*n*UT** concentration fixed at 1.9×10^{-5} M), aimed at the formation of mixed supramolecular architectures. As in chloroform, the absorption spectra show a gradual transition from pure OPV to a mixed OPV/perylene bisimide system. However, the fluorescence spectra indicate a much more dramatic decrease in OPV fluorescence (at $\lambda_{em}=512$ nm for **OPV3UT** and at $\lambda_{em}=556$ nm for **OPV4UT**) as compared with the situation in chloroform. This suggests the incorporation of **OPV4UT-PERY** into columnar aggregates of pure **OPV*n*UT** in which the perylene bisimide units are able to effectively quench the luminescence of the assembled OPVs. The enhanced quenching efficiency of the **OPV4UT** host relative to **OPV3UT** may be

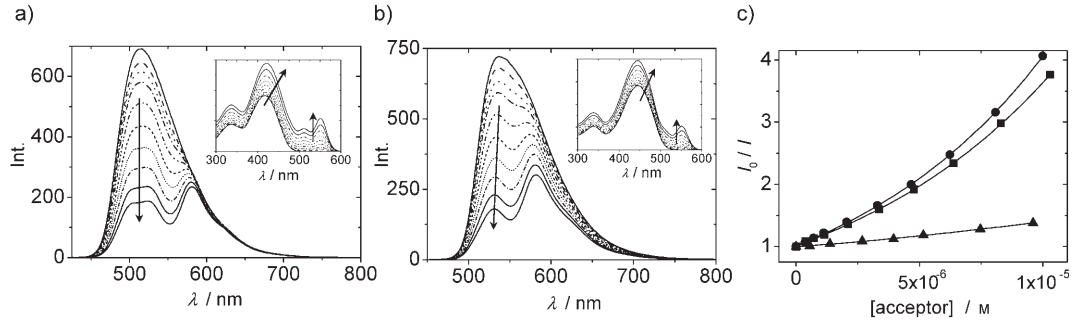

Figure 7. Fluorescence mixing experiments in chloroform at room temperature, performed by adding 0–35 mol% **OPV4UT-PERY** to a) **OPV3UT** ($\lambda_{exc}=409$ nm) and b) **OPV4UT** ($\lambda_{exc}=437$ nm, both donors fixed at 1.9×10^{-5} M). The insets show the UV/Vis spectra for the corresponding mixtures. c) Quenching behavior for **OPV3UT** (■) and for **OPV4UT** (●), monitored at $\lambda_{em}=515$ and 535 nm, respectively. This behavior is compared with **OPV3UT** quenching in the system **OPV3UT/OPV4UT** in chloroform at room temperature, monitored at $\lambda_{em}=513$ nm (▲). Lines to guide the eye.

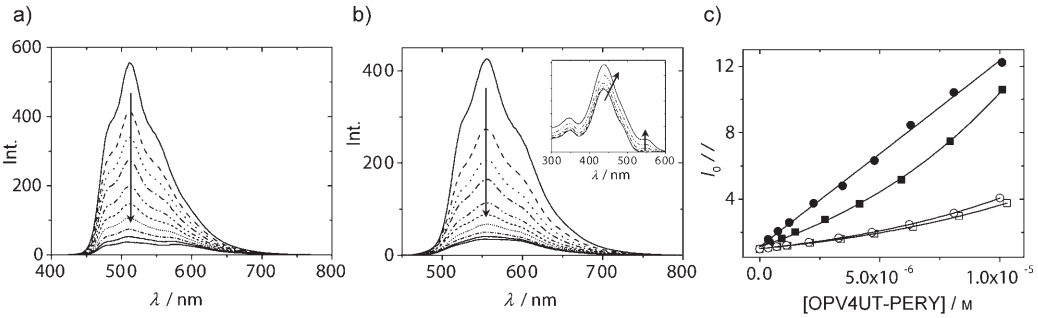

Figure 8. Mixing experiments in dodecane at room temperature, performed by adding a) 0–39 mol% **OPV4UT-PERY** to **OPV3UT** ($\lambda_{exc}=409$ nm) and b) 0–34 mol% **OPV4UT-PERY** to **OPV4UT** ($\lambda_{exc}=437$ nm, both donors fixed at 1.9×10^{-5} M). The inset shows the increase in UV/Vis absorption upon addition of 0–30 mol% acceptor. c) Quenching behavior for **OPV3UT** (■) and for **OPV4UT** (●) hosts, monitored at $\lambda_{em}=512$ and 556 nm, respectively. For comparison, the quenching behavior in chloroform is also shown (from Figure 7, corresponding open symbols, □ and ○). Lines to guide the eye.

caused by differences in the π–π stacking interactions with the acceptor.[32] The difference in quenching behaviour, represented by the slopes of the two lines (linear versus superlinear, respectively), is striking and may be a direct consequence of the presence of two acceptor molecules (**OPV4UT** and perylene bisimide) for the **OPV3UT** host. However, since the luminescence quantum yield of the perylene bisimide is much reduced in dodecane, interpretation of the spectra with regard to the situation observed in chloroform is difficult. Moreover, fluorescence quenching based on the number of acceptor molecules is less efficient than was observed for mixed helical assemblies of **OPV3UT/OPV4UT** in dodecane.[33] This decrease in energy-transfer efficiency along stacked chromophores may again be related to steric effects upon incorporation of **OPV4UT-PERY**.

Conclusion

By covalent attachment at its ureido position, **OPV*n*UT** has been functionalized with a perylene bisimide chromophore using a flexible pentamethylene spacer. The resulting donor–acceptor building block is characterized by efficient intramolecular energy transfer from OPV to perylene bisimide, yielding bathochromically shifted luminescence properties. In spite of the bulkiness of the perylene bisimide moiety, hydrogen-bonded dimers are formed in chloroform through quadruple hydrogen bonding of the self-complementary ureido-*s*-triazine arrays. These dimers were subsequently visualized on a graphite surface using STM. The STM images showed a striking bias-dependant contrast, revealing the relative orientation of the OPV and perylene bisimide units and their different electronic properties.

Whereas chirality has been incorporated into the side-chains of the molecular backbone, the oligomer self-assembles into architectures without preferred supramolecular helicity in dodecane. This process is probably dominated by the size of the appended perylene bisimide and the inherent flexibility of the connecting spacer. Unfortunately, the absence of detailed information on the internal structure of these assemblies makes an unequivocal assignment of the specific stacking arrangement difficult. Our data suggest that a successful design of ordered donor–acceptor co-assemblies with specific functionality based on a "double-cable" approach should encompass a certain degree of pre-organization.

Experimental Section

Methods and materials: ^{1}H and ^{13}C NMR spectra were recorded with a Varian Gemini (300 MHz for ^{1}H NMR and 75 MHz for ^{13}C NMR), a Varian Mercury (400 MHz for ^{1}H NMR and 100 MHz for ^{13}C NMR) or a Varian Unity Inova (500 MHz for ^{1}H NMR and 125 MHz for ^{13}C NMR) spectrometer. Chemical shifts are reported in ppm downfield from tetramethylsilane (TMS) at room temperature using $CDCl_3$ as solvent and internal standard unless otherwise indicated. Abbreviations used for splitting patterns are s = singlet, d = doublet, dd = double doublet, t = triplet, dt = double triplet, q = quartet, m = multiplet, and br = broad. IR spectra were recorded with a Perkin-Elmer 1600 FT-IR (UATR) spectrometer. Matrix-assisted laser desorption ionization time-of-flight mass spectrometry (MALDI-TOF MS) was performed with a PerSeptive Biosystems Voyager-DE PRO spectrometer using an α-cyano-4-hydroxycinnamic acid matrix. Electrospray ionization (ESI) mass spectrometry was performed with a Q/TOF Ultima GLOBAL mass spectrometer (Micromass, Manchester, UK) equipped with a Z-spray source. Elemental analyses were carried out using a Perkin-Elmer 2400 instrument. UV/Vis spectra were recorded with either a Perkin-Elmer Lambda 40P or a Perkin-Elmer Lambda 900 UV/Vis/NIR spectrometer, CD spectra with a JASCO J-600 spectropolarimeter (sensitivity, time constant, and scan-rate were chosen appropriately), fluorescence spectra with either a Perkin-Elmer LS-50B luminescence spectrometer or an Edinburgh Instrument FS920 double-monochromator spectrometer with a Peltier-cooled red-sensitive photomultiplier. A PTC-348WI Peltier-type temperature control system was used to measure variable-temperature CD spectra. A Peltier Temperature Programmer model 1 (PTP-1) was used to measure variable-temperature UV/Vis and fluorescence spectra. All solvents were of AR quality. Other reagents were purchased from Acros and Aldrich and were used without further purification. DMA and pyridine were dried over 4 Å molecular sieves. Bio-Beads S-X1 and S-X3 were obtained from Bio-Rad Laboratories.

Synthesis: 1,7-Bis(3,5-di-*tert*-butylphenoxy)perylene-3,4:9,10-tetracarboxylic dianhydride[11c] and **OPV4T**[16a] were prepared according to literature procedures.

***N*-(1-Ethylpropyl)-1,7-bis(3,5-di-*tert*-butylphenoxy)perylenedicarboxylic-3,4-anhydride 9,10-imide (1)**: 1,7-Bis(3,5-di-*tert*-butylphenoxy)perylene-3,4:9,10-tetracarboxylic dianhydride (1.0 g, 1.25 mmol), 1-ethylpropyla-

mine (0.13 g, 1.50 mmol, 1.2 equiv), and $Zn(OAc)_2$ (0.28 g, 1.50 mmol) were dissolved in dry *N*,*N*-dimethylacetamide (35 mL). The solution was degassed with N_2 for a period of 30 min and then placed in an argon atmosphere. The reaction mixture was refluxed for 3 h. After cooling to room temperature, the remaining starting compound was precipitated in diethyl ether, the solution was filtered, and the ether layer evaporated to dryness. The remaining solid was purified extensively by column chromatography (SiO_2, pentane/dichloromethane 2:3) yielding pure **1** (300 mg, 0.34 mmol, 28%) as a red solid. ^{1}H NMR: $\delta = 0.90$ (t, 6H; CH_2CH_3), 1.35 (s, 18H; $C(CH_3)_3$), 1.36 (s, 18H; $C(CH_3)_3$), 1.91 (m, 2H; CH_2), 2.21 (m, 2H; CH_2), 4.99 (m, 1H; CH), 7.02 (d, 2H; ArH) 7.04 (d, 2H; ArH), 7.38 (2t, 2H; ArH), 8.29 (s, 1H; ArH), 8.35 (s, 1H; ArH), 8.59 (d, 1H; ArH), 8.63 (d, 1H; ArH), 9.66 (d, 1H; ArH), 9.69 ppm (d, 1H; ArH); ^{13}C NMR: $\delta = 11.6$, 25.2, 31.62, 31.64, 35.4, 58.0, 114.4, 114.8, 117.6, 119.0, 120.10, 120.12, 122.1, 123.3, 124.97, 125.02, 127.1, 128.7, 129.5, 129.6, 129.7, 130.2, 132.1, 132.7, 135.3, 154.1, 154.2, 154.5, 154.6, 155.8, 156.9, 159.8, 159.9 ppm; IR: $\tilde{\nu} = 2962$, 2906, 2872, 1773, 1734, 1704, 1663, 1603, 1590, 1570, 1514, 1476, 1461, 1407, 1364, 1344, 1318, 1292, 1258, 1229, 1195, 1163, 1119, 1085, 1057, 1018, 948, 920, 900, 878, 870, 855, 809, 750, 707, 667 cm^{-1}; MALDI-TOF MS (869.43): *m*/*z*: 870.43 $[M+H]^+$; elemental analysis calcd (%) for $C_{57}H_{59}NO_7$: C 78.68, H 6.83, N 1.61; found: C 77.57, H 6.88, N 1.57.

***N*,*N*′-Bis(1-ethylpropyl)-1,7-bis(3,5-di-*tert*-butylphenoxy)perylene-3,4:9,10-tetracarboximide (1b)**: This molecule was obtained as a side-product in the synthesis of **1**, along with the 1,6 regioisomer(*) (~15%). It was used as a reference compound for optical studies. ^{1}H NMR: $\delta =$ 0.92 (t, 12H; CH_2CH_3), 1.37 (s, 36H; $C(CH_3)_3$), 1.93 (m, 4H; CH_2), 2.22 (m, 4H; CH_2), 5.02 (m, 2H; CH), 7.06 (d, 2H; ArH), 7.38 (t, 2H; ArH), 8.36 (8.26*) (s, 2H; ArH), 8.61 (8.69*) (d, 2H; ArH), 9.65 (9.60*) ppm (d, 2H; ArH); ^{13}C NMR: $\delta = 11.2$, 24.9, 31.3, 35.1, 57.5, 114.4, 119.4, 122.2, 123.1, 123.3, 123.7, 125.0, 128.6, 129.2, 130.0, 133.4, 153.6, 154.5, 155.8 ppm; IR: $\tilde{\nu} = 2962$, 2907, 2875, 1698, 1657, 1600, 1588, 1571, 1514, 1479, 1460, 1421, 1407, 1380, 1363, 1344, 1327, 1318, 1293, 1259, 1247, 1218, 1201, 1188, 1148, 1119, 1057, 1027, 1012, 1002, 954, 926, 916, 900, 858, 831, 811, 787, 750, 707, 660 cm^{-1}; MALDI-TOF MS (938.52): *m*/*z*: 938.58 $[M]^+$; elemental analysis calcd (%) for $C_{62}H_{70}N_2O_6$: C 79.29, H 7.51, N 2.98; found: C 78.91, H 7.54, N 2.93.

***N*-(1-Ethylpropyl)-*N*′-5-aminopentyl-1,7-bis(3,5-di-*tert*-butylphenoxy)perylene-3,4:9,10-tetracarboximide (2)**: Compound **1** (280 mg, 0.32 mmol), 1,5-pentanediamine (0.33 g, 3.22 mmol), and $Zn(OAc)_2$ (0.12 g, 0.64 mmol) were dissolved in dry *N*,*N*-dimethylacetamide (4 mL). The solution was degassed with N_2 for 10 min and then placed in an argon atmosphere. The mixture was subsequently stirred at 50 °C for 2 h and after cooling to room temperature, the solvent was removed in vacuo. Pure **2** (200 mg, 0.21 mmol, 65%) was obtained after column chromatography (SiO_2, dichloromethane then dichloromethane/methanol 95:5). ^{1}H NMR: $\delta = 0.84$ (t, 6H; CH_2CH_3), 1.30 (s, 36H; $C(CH_3)_3$), 1.41 (m, 2H; $NCH_2CH_2CH_2$), 1.57 (m, 2H; $CH_2CH_2NH_2$), 1.71 (m, 2H; NCH_2CH_2), 1.86 (m, 2H; $CHCH_2$), 1.97, (s, 2H; NH_2), 2.15 (m, 2H; $CHCH_2$), 2.72 (t, 2H; CH_2NH_2), 4.12 (t, 2H; NCH_2), 4.95 (m, 1H; CH), 7.00 (s, 4H; ArH), 7.33 (2t, 2H; ArH), 8.31 (s, 2H; ArH), 8.58 (2d, 2H; ArH), 9.65 ppm (2d, 2H; ArH); ^{13}C NMR: $\delta = 10.4$, 23.0, 23.9, 26.3, 26.8, 28.7, 30.4, 34.1, 38.5, 39.1, 56.6, 113.2, 118.4, 120.6, 121.4, 121.8, 122.0, 122.3, 123.0, 123.4, 123.8, 127.5, 127.8, 128.8, 131.9, 132.3, 152.6, 152.7, 153.4, 153.5, 154.5, 154.8, 161.6, 162.1 ppm; IR: $\tilde{\nu} = 3387$, 3166, 3068, 2962, 2873, 1698, 1657, 1601, 1589, 1514, 1459, 1420, 1407, 1363, 1332, 1293, 1262, 1213, 1202, 1188, 1118, 1057, 956, 899, 871, 856, 811, 753, 708 cm^{-1}; MALDI-TOF MS (953.53): *m*/*z*: 954.62 $[M+H]^+$.

***N*-(1-Ethylpropyl)-*N*′-(5-isocyanatopentyl)-1,7-bis(3,5-di-*tert*-butylphenoxy)perylene-3,4:9,10-tetracarboximide (3)**: Di-*tert*-butyl tricarbonate (68 mg, 0.26 mmol) was dissolved in dry dichloromethane (6 mL) under argon. A solution of **2** (0.2 g, 0.21 mmol) in dry dichloromethane (13 mL) was added dropwise and the resulting mixture was stirred for 10 min after which the solvent was evaporated in vacuo. FTIR spectroscopy revealed the formation of the corresponding isocyanate **3** ($\tilde{\nu} = 2274$ cm^{-1}), which was used without further purification. ^{1}H NMR: $\delta = 0.89$ (t, 6H; CH_2CH_3), 1.34 (s, 36H; $C(CH_3)_3$), 1.49 (m, 2H; $NCH_2CH_2CH_2$), 1.63–1.81 (m, 4H; CH_2CH_2NCO, NCH_2CH_2), 1.90 (m, 2H; $CHCH_2$), 2.20 (m, 2H; $CHCH_2$), 3.31 (t, 2H; CH_2NCO), 4.16 (t, 2H; NCH_2), 5.00 (m, 1H; NCH), 7.03 (s, 4H; ArH), 7.35 (t, 2H; ArH), 8.34 (s, 2H; ArH), 8.62 (2d, 2H; ArH), 9.67 ppm (2d, 2H; ArH).

2-Amino-4-{5-[9,10-(1-ethylpropylimidodicarbonyl)-1,7-bis(3,5-di-*tert*-butylphenoxy)perylene-3,4-dicarboximido]pentylureido}-6-[(*E*,*E*,*E*)-4-(4-{4-[3,4,5-tris(dodecyloxy)styryl]-2,5-bis[(*S*)-2-methylbutoxy]styryl}-2,5-bis[(*S*)-2-methylbutoxy]styryl)phenyl]-*s*-triazine (OPV4UT-PERY): **OPV4T** (0.3 g, 0.22 mmol) was dissolved in dry pyridine (2 mL) under argon and refluxed. A solution of **3** (0.205 g, 0.21 mmol) in dry pyridine (2 mL) was added and the mixture was concentrated to ≈2 mL by opening the reaction vessel. After stirring for 16 h, the solvent was removed in vacuo and the mixture purified by chromatography (SiO_2, dichloromethane, then dichloromethane/ethanol 98.5:1.5). After precipitation in methanol and size-exclusion chromatography (Bio-Beads S-X1, THF) pure **OPV4UT-PERY** (80 mg, 0.034 mmol, 15%) was obtained as a red solid. ^{1}H NMR: $\delta = 0.86$–0.95 (m, 15H; $(CH_2)_8CH_3$, $NCHCH_2CH_3$), 0.99–1.04 (m, 12H; $CHCH_3$), 1.10–1.17 (m, 12H; $CHCH_3$), 1.28–1.56 (m, 90H; $(CH_2)_8CH_3$, $CHCH_3$, $C(CH_3)_3$, $NCH_2(CH_2)_2CH_2CH_2NCON$), 1.43–1.56 (m, 6H; $OCH_2CH_2CH_2$), 1.58–2.00 (m, 20H; $CHCH_3$, OCH_2CH_2, $CHCH_3$, $NCH_2(CH_2)_2CH_2CH_2NCON$, $NCHCH_2CH_3$), 2.12–2.17 (m, 2H; $NCHCH_2CH_3$), 3.32 (t, 2H; CH_2NCON), 3.87–4.05 (m, 14H; OCH_2), 4.16 (t, 2H; NCH_2), 4.96 (m, 1H; NCH), 5.30 (br, 1H; ArN*H*H), 6.75 (s, 2H; ArH), 6.99 (s, 2H; ArH), 7.03 (s, 2H; ArH), 7.04 (d, 1H; C*H*=CH), 7.09 (s, 1H; ArH), 7.11 (d, 1H; C*H*=CH), 7.16 (s, 1H; ArH), 7.16 (d, 1H; C*H*=CH), 7.17 (d, 1H; CH=C*H*), 7.31 (s, 1H; ArH), 7.34 (s, 1H; ArH), 7.39 (d, 1H; CH=C*H*), 7.47 (s, 2H; ArH), 7.56 (d, 1H; CH=C*H*), 7.60 (d, 2H; ArH), 8.13 (d, 2H; ArH), 8.29 (s, 1H; ArH), 8.32 (s, 1H; ArH), 8.52 (2d, 2H; ArH), 9.19 (br, 1H; ArNH*H*), 9.62 (2d, 2H; ArH), 9.62 (br, 1H; NH), 9.84 ppm (br, 1H; NH); ^{13}C NMR: $\delta =$ 11.4, 11.46, 11.54, 11.6, 14.2, 16.8, 16.90, 16.92, 22.7, 24.1, 25.0, 26.2, 26.42, 26.44, 27.4, 29.0, 29.42, 29.44, 29.5, 29.68, 29.71, 29.74, 29.76, 29.79, 29.81, 30.35, 30.40, 31.2, 31.4, 31.6, 32.0, 35.0, 35.1, 35.16, 35.18, 35.20, 39.5, 40.3, 57.6, 69.1, 73.6, 74.1, 74.2, 74.4, 105.1, 109.5, 109.8, 110.5, 110.9, 114.2, 114.4, 119.3, 119.4, 121.9, 122.4, 122.5, 122.9, 123.3, 123.4, 123.5, 123.6, 124.9, 125.1, 125.7, 126.1, 126.5, 126.9, 127.3, 127.6, 128.2, 128.7, 128.8, 129.0, 129.3, 129.4, 130.0, 133.3, 133.5, 133.8, 134.2, 138.2, 142.1, 150.9, 151.1, 151.2, 151.5, 153.3, 153.7, 154.8, 155.6, 155.8, 156.1, 163.1, 163.5, 167.2, 170.2 ppm; IR: $\tilde{\nu} = 3499$, 3292, 3196, 3129, 3057, 2958, 2924, 2855, 1697, 1659, 1602, 1590, 1571, 1528, 1506, 1465, 1420, 1407, 1364, 1333, 1294, 1262, 1203, 1170, 1116, 1053, 1011, 960, 915, 900, 855, 811, 773, 753, 708 cm^{-1}. ESI-MS (2369.58): *m*/*z*: 2370.73 $[M+H]^+$.

Scanning tunneling microscopy: All STM experiments were performed at room temperature and under ambient conditions. The STM images presented here were obtained at the liquid/solid interface using a Discoverer scanning tunneling microscope (Topometrix Inc., Santa Barbara, CA) along with an external pulse/function generator (model HP 8111A). Low-current experiments were performed using a multimode Nanoscope IV instrument (Digital Instruments Co., Santa Barbara, CA). STM tips were electrochemically etched from Pt/Ir wire (80/20, diameter 0.2 nm) in an aqueous 2N KOH/6N NaCN solution. Highly oriented pyrolytic graphite (HOPG; grade ZYB, advanced Ceramics Inc., Cleveland, OH) was used as the substrate. A drop of a solution of **OPV4UT-PERY** (0.5 mg mL^{-1}) in 1,2,4-trichlorobenzene (Aldrich) was applied to a freshly cleaved surface of HOPG. STM images were acquired in the variable current mode by scanning the STM tip immersed in solution at a negative sample bias (electrons tunnel from the sample to the tip). The measured tunneling currents were converted into a gray scale: black (white) refers to a low (high) measured tunneling current. After successful imaging of the monolayer, an atomically resolved image of the graphite substrate was recorded at exactly the same location with identical scanning parameters except for the sample bias. The images were corrected for scanner drift by using SPIP software.[34] (Image Metrology ApS) with graphite as the calibration grid. Only images containing a small drift were used for analysis.

Acknowledgements

The authors in Eindhoven thank the Netherlands Organization for Scientific Research (NWO-CW). Dr. Edwin Beckers is acknowledged for the PIA measurements. The authors in Leuven thank the Federal Science Policy through IUAP-V-03 and the Institute for the Promotion of Innovation by Science and Technology in Flanders (IWT). Support from the Fund for Scientific Research-Flanders (FWO) and K.U.Leuven is also acknowledged.

[1] F. J. M. Hoeben, P. Jonkheijm, E. W. Meijer, A. P. H. J. Schenning, *Chem. Rev.* **2005**, *105*, 1491–1546.
[2] *Supramolecular dye chemistry* (Ed.: F. Würthner), *Top. Curr. Chem.* 258, Springer, New York **2005**.
[3] T. Steiner, *Angew. Chem.* **2002**, *114*, 50–80; *Angew. Chem. Int. Ed.* **2002**, *41*, 48–76.
[4] L. Prins, D. Reinhoudt, P. Timmerman, *Angew. Chem.* **2001**, *113*, 2446–2492; *Angew. Chem. Int. Ed.* **2001**, *40*, 2383–2426.
[5] a) J. V. Barth, J. Weckesser, C. Cai, P. Günter, L. Bürgi, O. Jeandupeux, K. Kern, *Angew. Chem.* **2000**, *112*, 1285–1288; *Angew. Chem. Int. Ed.* **2000**, *39*, 1230–1234; b) S. De Feyter, F. C. De Schryver, *Chem. Soc. Rev.* **2003**, *32*, 139–150; c) S. De Feyter, F. C. De Schryver, *Top. Curr. Chem.* **2005**, *258*, 205–255.
[6] M. Ward, *Chem. Soc. Rev.* **1997**, *26*, 365–375.
[7] a) F. Jäckel, M. D. Watson, K. Müllen, J. P. Rabe, *Phys. Rev. Lett.* **2004**, *92*, 188303; b) N. Tchebotareva, X. Yin, M. D. Watson, P. Samorì, J. P. Rabe, K. Müllen, *J. Am. Chem. Soc.* **2003**, *125*, 9734–9739; c) P. Samori, X. Yin, N. Tchebotareva, Z. H. Wang, T. Pakula, F. Jäckel, M. D. Watson, A. Venturini, K. Müllen, J. P. Rabe, *J. Am. Chem. Soc.* **2004**, *126*, 3567–3575; d) P. Samori, A. Fechtenkötter, E. Reuther, M. D. Watson, N. Severin, K. Müllen, J. P. Rabe, *Adv. Mater.* **2006**, *18*, 1317–1321; e) E. Mena-Osteritz, P. Bäuerle, *Adv. Mater.* **2006**, *18*, 447–451.
[8] a) A. Miura, Z. Chen, H. Uji-I, S. De Feyter, M. Zdanowska, P. Jonkheijm, A. P. H. J. Schenning, E. W. Meijer, F. Würthner, F. C. De Schryver, *J. Am. Chem. Soc.* **2003**, *125*, 14968–14969; b) H. Uji-i, A. Miura, A. P. H. J. Schenning, E. W. Meijer, Z. Chen, F. Würthner, F. C. De Schryver, M. van der Auweraer, S. De Feyter, *ChemPhysChem* **2005**, *6*, 2389–2395; c) S. De Feyter, A. Miura, S. Yao, Z. Chen, F. Würthner, P. Jonkheijm, A. P. H. J. Schenning, E. W. Meijer, F. C. De Schryver, *Nano Lett.* **2005**, *5*, 77–81.
[9] R. E. Martin, F. Diederich, *Angew. Chem.* **1999**, *111*, 1140–1469; *Angew. Chem. Int. Ed.* **1999**, *38*, 1351–1377.
[10] a) R. A. Cormier, B. A. Gregg, *J. Phys. Chem. B* **1997**, *101*, 11004–11006; b) R. A. Cormier, B. A. Gregg, *Chem. Mater.* **1998**, *10*, 1309–1319; c) F. Würthner, C. Thalacker, S. Diele, C. Tschierske, *Chem. Eur. J.* **2001**, *7*, 2245–2253; d) F. Würthner, C. Thalacker, A. Sautter, *Adv. Mater.* **1999**, *11*, 754–758; e) F. Würthner, C. Thalacker, A. Sautter, W. Schärtl, W. Ibach, O. Hollricher, *Chem. Eur. J.* **2000**, *6*, 3871–3885; f) C. W. Struijk, A. B. Sieval, J. E. J. Dakhorst, M. van Dijk, P. Kimkes, R. B. M. Koehorst, H. Donker, T. J. Schaafsma, S. J. Picken, A. M. van de Craats, J. M. Warman, H. Zuilhof, E. J. R. Sudhölter, *J. Am. Chem. Soc.* **2000**, *122*, 11057–11066.
[11] a) E. E. Neuteboom, E. H. A. Beckers, S. C. J. Meskers, E. W. Meijer, R. A. J. Janssen, *Org. Biomol. Chem.* **2003**, *1*, 198–203; b) F. Würthner, A. Sautter, *Org. Biomol. Chem.* **2003**, *1*, 240–243; c) T. van der Boom, R. T. Hayes, Y. Zhao, P. J. Bushard, E. A. Weiss, M. R. Wasielewski, *J. Am. Chem. Soc.* **2002**, *124*, 9582–9590.
[12] a) W. Wang, L.-S. Li, G. Helms, H.-H. Zhou A. D. Q. Li, *J. Am. Chem. Soc.* **2003**, *125*, 1120–1121; b) A. D. Q. Li, W. Wang, L.-Q. Wang, *Chem. Eur. J.* **2003**, *9*, 4594–4601.
[13] a) L. Schmidt-Mende, A. Fechtenkötter, K. Müllen, E. Moons, R. H. Friend, J. D. MacKenzie, *Science* **2001**, *293*, 1119–1122; b) C. W. Tang, *Appl. Phys. Lett.* **1986**, *48*, 183–185; c) A. J. Breeze, A. Salomon, D. S. Ginley, B. A. Gregg, H. Tillmann, H.-H. Hörhold, *Appl. Phys. Lett.* **2002**, *81*, 3085–3087; d) L. Y. Park, D. G. Hamilton, E. A. McGehee, K. A. McMenimen, *J. Am. Chem. Soc.* **2003**, *125*, 10586–10590.
[14] a) C. Ludwig, B. Gompf, J. Petersen, R. Strohmaier, W. Eisenmenger, *Z. Phys. B* **1994**, *93*, 365–373; b) Y. Kaneda, M. E. Stawasz, D. L. Sampson, B. A. Parkinson, *Langmuir* **2001**, *17*, 6185–6195; c) J. C. Swarbrick, J. Ma, J. A. Theobald, N. S. Oxtoby, J. N. O'Shea, N. R. Champness, P. H. Beton, *J. Phys. Chem. B* **2005**, *109*, 12167–12174.
[15] a) A. Gesquière, P. Jonkheijm, A. P. H. J. Schenning, E. Mena-Osteritz, P. Bäuerle, S. De Feyter, F. C. De Schryver, E. W. Meijer, *J. Mater. Chem.* **2003**, *13*, 2164–2167; b) P. Jonkheijm, A. Miura, M. Zdanowska, F. J. M. Hoeben, S. De Feyter, A. P. H. J. Schenning, F. C. De Schryver, E. W. Meijer, *Angew. Chem.* **2004**, *116*, 76–88; *Angew. Chem. Int. Ed.* **2004**, *43*, 74–78; c) A. Miura, P. Jonkheijm, S. De Feyter, A. P. H. J. Schenning, E. W. Meijer, F. C. De Schryver, *Small* **2005**, *1*, 131–137; d) A. Gesquière, P. Jonkheijm, F. J. M. Hoeben, A. P. H. J. Schenning, S. De Feyter, F. C. De Schryver, E. W. Meijer, *Nano Lett.* **2004**, *4*, 1175–1179.
[16] a) A. P. H. J. Schenning, P. Jonkheijm, E. Peeters, E. W. Meijer, *J. Am. Chem. Soc.* **2001**, *123*, 409–416; b) P. Jonkheijm, F. J. M. Hoeben, R. Kleppinger, J. van Herrikhuyzen, A. P. H. J. Schenning, E. W. Meijer, *J. Am. Chem. Soc.* **2003**, *125*, 15941–15949.
[17] a) E. Peeters, P. A. van Hal, S. C. J. Meskers, R. A. J. Janssen, E. W. Meijer, *Chem. Eur. J.* **2002**, *8*, 4470–4474; b) A. Syamakumari, A. P. H. J. Schenning, E. W. Meijer, *Chem. Eur. J.* **2002**, *8*, 3353–3361; c) A. P. H. J. Schenning, J. van Herrikhuyzen, P. Jonkheijm, Z. Chen, F. Würthner, E. W. Meijer, *J. Am. Chem. Soc.* **2002**, *124*, 10252–10253; d) F. Würthner, Z. Chen, F. J. M. Hoeben, P. Osswald, C.-C. You, P. Jonkheijm, J. van Herrikhuyzen, A. P. H. J. Schenning, P. P. A. M. van der Schoot, E. W. Meijer, E. H. A. Beckers, S. C. J. Meskers, R. A. J. Janssen, *J. Am. Chem. Soc.* **2004**, *126*, 10611–10618.
[18] 400 MHz ^{1}H NMR spectroscopy clearly showed the presence of the 1,6- and 1,6,7-regioisomers in the crude reaction mixture. We have discovered that these isomers can be removed in the case of perylene bisimides with two different substituents at the *N*-imide positions. In the literature, perylenes substituted at the bay positions are often prepared along with small amounts of regioisomers, although this is hardly ever mentioned by the authors, see: a) U. Rohr, C. Kohl, K. Müllen, A. van de Craats, J. Warman, *J. Mater. Chem.* **2001**, *11*, 1789–1799; b) F. Würthner, V. Stepanenko, Z. Chen, C. R. Saha-Moller, N. Kocher, D. Stalke, *J. Org. Chem.* **2004**, *69*, 7933–7939.
[19] H. W. I. Peerlings, E. W. Meijer, *Tetrahedron Lett.* **1999**, *40*, 1021–1024.
[20] Since the dielectric constant of 1,2,4-trichlorobenzene [$\varepsilon = 2.24$ (25 °C)] is lower than that of chloroform [$\varepsilon = 4.81$ (20 °C)] we expect a slightly higher dimerization constant in the former solvent.
[21] Based upon the dimerization constant of **OPV4UT** ($21000\,\mathrm{M}^{-1}$), which is an upper limit for the dimerization constant of **OPV4UT-PERY**, a maximum 70% of the molecules appear as dimers in solution.
[22] For **OPV4UT-PERY**, the lattice constants of a 2D unit cell of oblique symmetry were estimated to be $a = 2.66 \pm 0.05$, $b = 5.9 \pm 0.2$ nm, and $\gamma = 71 \pm 2°$ by extrapolation. For **OPV4UT**, these parameters are $a = 1.99 \pm 0.05$, $b = 5.4 \pm 0.2$ nm, and $\gamma = 85 \pm 3°$.
[23] The substitution at the bay area of the PERY unit (two *tert*-butylphenoxy groups) is different from that in the donor–acceptor–donor (DAD) triads previously investigated (four *tert*-butylphenoxy groups). However, we do not anticipate big differences in the bias dependence as unsubstituted perylene bisimide units show a bias-dependent behavior identical to that of the DAD triad with four *tert*-butylphenoxy groups (see ref. [8b]).
[24] L. M. Herz, C. Daniel, C. Silva, F. J. M. Hoeben, A. P. H. J. Schenning, E. W. Meijer, R. H. Friend, R. T. Phillips, *Phys. Rev. B* **2003**, *68*, 045203/1–045203/7.
[25] E. E. Neuteboom, P. A. van Hal, R. A. J. Janssen, *Chem. Eur. J.* **2004**, *10*, 3907–3918.
[26] a) F. Würthner, C. Thalacker, A. Sautter, *Adv. Mater.* **1999**, *11*, 754–758; b) M. J. Ahrens, L. E. Sinks, B. Rybtchinski, W. Liu, B. A. Jones, J. M. Giaimo, A. V. Gusev, A. J. Goshe, D. M. Tiede, M. R. Wasielewski, *J. Am. Chem. Soc.* **2004**, *126*, 8284–8294.

[27] The perylene bisimide emission maximum in dodecane is shifted hypsochromically from that in chloroform whereas excitonic coupling between π-conjugated chromophores should yield a distinct bathochromic luminescence shift. The temperature-dependent data, however, do exhibit a bathochromic shift upon self-assembly. The blue shift observed upon going from chloroform to dodecane may be due to specific environmental or packing parameters.
[28] See ref. [16b] for a simulated model based on quantum-chemical calculations.
[29] J. Wu, M. Baumgarten, M. G. Debije, J. M. Warman, K. Müllen, *Angew. Chem.* **2004**, *116*, 5445–5449; *Angew. Chem. Int. Ed.* **2004**, *43*, 5331–5335.
[30] E. H. A. Beckers, S. C. J. Meskers, A. P. H. J. Schenning, Z. Chen, F. Würthner, R. A. J. Janssen, *J. Phys. Chem. A* **2004**, *108*, 6933–6937.
[31] Selective excitation of perylene bisimide at $\lambda_{exc} = 540$ nm (data not shown) leads to a gradual increase in its luminescence at $\lambda_{em} = 580$ nm with increasing **OPV4UT-PERY** concentration, which is similar for both systems.
[32] This is corroborated by the measured Cotton effects (data not shown), which are totally lost for **OPV3UT** or strongly decrease in intensity for **OPV4UT** upon addition of **OPV4UT-PERY**.
[33] F. J. M. Hoeben, L. M. Herz, C. Daniel, P. Jonkheijm, A. P. H. J. Schenning, C. Silva, S. C. J. Meskers, D. Beljonne, R. T. Phillips, R. H. Friend, E. W. Meijer, *Angew. Chem.* **2004**, *116*, 2010–2013; *Angew. Chem. Int. Ed.* **2004**, *43*, 1976–1979.
[34] http://www.imagemet.com.

Received: May 9, 2006
Published online: September 8, 2006

